

## EMERGING POLLUTANTS PHOTOCATALYSIS: EFFICIENT DEGRADATION USING $\text{Cu}_2\text{S}/\text{ZnO}$ NANOSTRUCTURES

Ikaro Tessaro<sup>1</sup>, Paula M. R. M. Santos<sup>1</sup>, Luiza F. Pinheiro<sup>1</sup>, Flavio H. C. Boldrin<sup>1</sup>, Laila G. Andrade<sup>1</sup>, Cesar A. F. M. P. Lico<sup>1</sup>, Lucas H. Cardia<sup>1</sup>, Bruno H. B. Silva<sup>1</sup>, Nicolas P. Moraes<sup>2</sup> & Liana A. Rodrigues<sup>1\*</sup>

<sup>1</sup>Escola de Engenharia de Lorena-EEL/USP, Estrada Municipal do Campinho S/N, CEP 12602-810, Lorena, São Paulo, Brazil.

<sup>2</sup>São Carlos Institute of Chemistry, University of São Paulo, Av. Trab. São Carlense, 400 - Parque Arnold Schimidt, São Carlos - SP, 13566-590

\* Corresponding author's email address: liana.r@usp.br

### ABSTRACT

In the field of environmental biotechnology, efforts to identify and degrade emerging micropollutants through advanced oxidative processes have proven both promising and essential. The study investigates the potential of copper sulfide-based photocatalysts, specifically  $\text{Cu}_2\text{S}$ , for degrading environmental pollutants such as sulfamethazine and salicylic acid in aquatic settings. The synthesis process involved creating composites of  $\text{Cu}_2\text{S}$  and  $\text{ZnO}$ , characterized by X-ray diffraction and FTIR, which confirmed distinct crystalline structures and interactions between  $\text{Cu}_2\text{S}$  and  $\text{ZnO}$ . Photocatalytic tests in a 0.5 L reactor under simulated sunlight conditions demonstrated effective pollutant degradation. Microscopy and EDS mapping indicated a uniform distribution of elements, essential for efficient charge transfer in heterojunctions, thereby enhancing photocatalytic performance. The integration of  $\text{Cu}_2\text{S}$  with  $\text{ZnO}$  not only improves charge separation but also increases visible light absorption, highlighting its potential for environmental applications. These results underscore the promise of  $\text{Cu}_2\text{S}-\text{ZnO}$  composites as advanced photocatalysts, validated by consistent outcomes in structural analysis and photocatalytic efficiency tests, making them suitable for sustainable pollution control technologies.

**Keywords:** Photocatalysis. Copper Sulfide. Zinc Oxide. Pollutant Degradation. Heterojunctions.

## 1 INTRODUCTION

The growing concern about environmental pollution has driven research into low-cost semiconductors, especially in heterogeneous photocatalysis. Copper sulfide, such as  $\text{Cu}_2\text{S}$  and  $\text{CuS}$ , stands out as a promising catalyst due to its non-toxicity and distinctive electronic properties. These semiconductors have been investigated for their effectiveness in pollutant photodegradation processes<sup>1</sup>.

Environmental biotechnology increasingly recognizes the importance of sophisticated techniques to identify and break down emerging micropollutants. Advanced oxidative processes have shown great promise in addressing the challenges of environmental pollution<sup>1-2</sup>. These techniques not only improve the efficiency of removal and degradation of persistent substances, but also support better waste management practices that align with the principles of environmental conservation and public safety<sup>2</sup>. Heterogeneous photocatalysis is a promising method for remediating pharmaceuticals, demonstrating high efficiency in the degradation and mineralization of various emerging pollutants<sup>2</sup>. In this technique, photocatalysts are irradiated with light, exciting electrons from the valence band (VB) to the conduction band (CB) of semiconductors. The resulting vacancy in the VB and the electron in the CB generate active radicals in an aqueous medium, which act as precursors for the degradation reactions of pollutants<sup>3</sup>.

Recent studies have explored the photocatalytic efficacy of  $\text{ZnO}$  and  $\text{Cu}_2\text{S}$  semiconductors in the presence of g-C<sub>3</sub>N<sub>4</sub> and the piezo-photocatalytic efficiency of the  $\text{CuS}/\text{ZnO}$  composite<sup>4</sup>. Direct electron transfer from the valence band of g-C<sub>3</sub>N<sub>4</sub> to  $\text{CuS}$ , resulting in partial reduction of  $\text{CuS}$  to  $\text{Cu}_2\text{S}$ , promoted charge separation<sup>5</sup>. Ultrasonic assistance significantly increased photocatalytic activity, while the formation of type II heterojunction with  $\text{ZnO}$  improved charge separation, and  $\text{CuS}$  contributed to greater visible light absorption<sup>6</sup>. Among the environmentally relevant compounds in this contamination process, sulfamethazine (SMZ) and salicylic acid (AS) are observed as persistent pollutants with high disruptive potential. They persist in the aquatic environment, negatively impacting the ecosystem by being toxic to some organisms and contributing to bacterial resistance, among other effects<sup>7</sup>.

Given the increasing demand for efficient and sustainable catalytic solutions, this study aims to investigate the synthesis and characterization of copper sulfide-based photocatalysts ( $\text{Cu}_2\text{S}$ )<sup>6</sup>. The main objective is to understand the influence of these materials on the effectiveness of advanced pollutant photodegradation processes in aqueous environments. This research seeks to contribute to the development of environmentally friendly and innovative catalytic technologies<sup>7</sup>.

## 2 MATERIAL & METHODS

For the synthesis of the materials, unary  $\text{Cu}_2\text{S}$  was initially prepared by dissolving predefined quantities of copper(II) nitrate trihydrate ( $\text{Cu}(\text{NO}_3)_2 \cdot 3\text{H}_2\text{O}$ , 99% w/w, CAS No. 10031-43-3) in 100 mL of deionized water, followed by the addition of stoichiometric amounts of ammonium sulfide  $(\text{NH}_4)_2\text{S}$ , 20% w/w solution. This mixture was stirred using a magnetic stirrer at room temperature. The resulting precipitates were washed with deionized water until the filtrate was free of chloride ions and reached a neutral pH. The washed materials were dried in an oven at 100 °C for 24 hours, then ground and sieved using a 325-mesh

analytical sieve. For the binary materials, 8.098 g of zinc chloride ( $\text{ZnCl}_2$ , 97% w/w, CAS No. 7646-85-7) were dissolved in 50 mL of deionized water using a magnetic stirrer at room temperature, and 0.375 g of unary  $\text{Cu}_2\text{S}$  material was dispersed, corresponding to a mass fraction of 7.5% by synthesis. The ternary material precipitation was induced by adding 50 mL of potassium hydroxide (KOH) solution (85% w/w, CAS No. 1310-58-3), with a predefined concentration of 7.197 g. The resulting precipitates were washed with deionized water until the filtrate was chloride-free and neutral in pH. The washed materials were dried in an oven at 100 °C for 24 hours, ground, and sieved using a 325-mesh analytical sieve. Subsequently, the materials were calcined in a muffle furnace at 600 °C for 30-minute, with a heating rate of 10 °C  $\text{min}^{-1}$  in a nitrogen-rich atmosphere (flow rate of 0.5 L  $\text{min}^{-1}$ ).

The characterization of the materials was performed using X-ray diffraction (XRD) and Fourier-transform infrared spectroscopy (FTIR). XRD identified the crystalline phases using a PANalytical Empyrean device with  $\text{CuK}\alpha$  radiation, covering the range of 20 to 70°. The chemical structure was analyzed with a Perkin Elmer Frontier spectrometer, operating in the range of 4000 to 500  $\text{cm}^{-1}$ , with a resolution of 4  $\text{cm}^{-1}$ . For morphological and compositional analysis, scanning microscopy and energy-dispersive spectroscopy (EDS) were used. EDS, using an Oxford Swift ED3000 spectrometer, provided qualitative and quantitative identification of the constituent elements, offering a comprehensive characterization of the studied materials.

Photocatalytic Evaluation Tests to assess the photocatalytic activity of the materials were conducted in a 0.5 L reactor, with constant magnetic stirring and temperature controlled at 25°C. Each test involved adding 0.1 g of the evaluated photocatalyst and 0.5 L of a solution containing 10  $\text{mg L}^{-1}$  of either salicylic acid (SA) or sulfamerazine (SMZ). The reactor was kept in the dark to achieve adsorption-desorption equilibrium between the pollutant and the catalyst. After equilibrium was reached, the samples were exposed to irradiation from a 300 W lamp to simulate sunlight radiation. The concentration of SA was measured with a UV-Vis spectrophotometer at 296 nm, and SMZ at 250 nm, after filtering the samples. Samples were collected at 15 minutes intervals initially, followed by 30 minutes intervals, over a period of 300 minutes or until complete degradation of the pollutant.

### 3 RESULTS & DISCUSSION

The characterizations are presented in the following section, accompanied by photocatalytic applications in degradation tests. The physicochemical analysis included evaluations by XRD and FTIR, while morphological and structural evaluations were performed using SEM and EDS.

X-ray diffraction (XRD) provided information on the structure and crystallinity of the unary materials, as shown in the diffractogram in Figures 1A and 1B. The peaks and bands of interest in the synthesized materials were identified with reference to the ICDD codes from the literature, according to the High Score Plus database, and FTIR in Figure 1C.

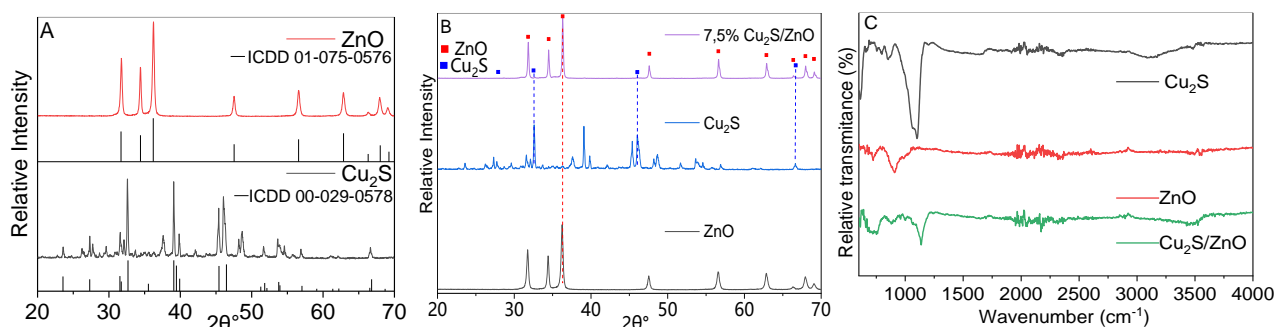


**Figure 1** (a) and (b) XRD diffractograms comparing with ICDD codes, and (c) FTIR spectra of the synthesized materials.

Figure 1 (a) and (b) shows the X-ray diffraction (XRD) patterns for the unary materials  $\text{ZnO}$  and  $\text{Cu}_2\text{S}$ , revealing their crystalline structures and corresponding crystallographic planes.  $\text{ZnO}$  exhibits characteristic hexagonal wurtzite peaks at  $2\theta$  positions such as 31.84° to 69.26°, aligning with planes like (100), (002), and (101).  $\text{Cu}_2\text{S}$  displays peaks at 32.66° to 66.71°, corresponding to planes including (103) and (200). These diffraction patterns confirm the distinct crystalline structures of  $\text{ZnO}$  and  $\text{Cu}_2\text{S}$ , with data consistent with theoretical standards (ICDD), validating the composition and structural integrity of the synthesized materials<sup>10</sup>.

The FTIR spectra on Figure 1 (c), of the synthesized materials reveal several characteristic absorption bands. In ternary materials with varying amounts of  $\text{Cu}_2\text{S}$ , a peak at 1380  $\text{cm}^{-1}$  indicates Cu–S stretching in  $\text{Cu}_2\text{S}/\text{ZnO}$  composites. Bands at 1466  $\text{cm}^{-1}$  correspond to methylene bending vibrations, and at 719  $\text{cm}^{-1}$  to Cu–S stretching. Different tannin quantities affect the intensity of O–C and C–H stretching bands, likely due to tannin polymerization. For materials calcined at different temperatures, peaks at 3447, 3499, and 3502  $\text{cm}^{-1}$  reflect O–H stretching vibrations, indicative of adsorbed water and hydroxyl groups, with intensities decreasing as calcination temperature increases. Comparative analysis of ternary, binary, and unary materials shows distinct Zn–O stretching peaks in  $\text{ZnO}$ , with  $\text{Cu}_2\text{S}$  incorporation confirmed by the presence of a 1380  $\text{cm}^{-1}$  peak in composites containing  $\text{Cu}_2\text{S}$ . These findings underscore strong interactions between  $\text{Cu}_2\text{S}$  nanoparticles and the  $\text{ZnO}$  matrix<sup>11</sup>.

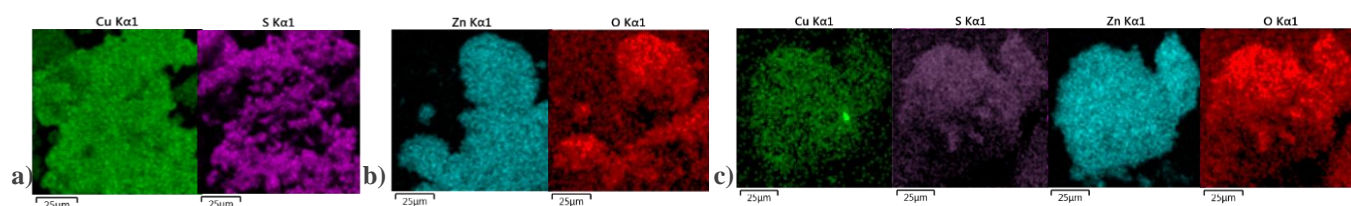


**Figure 2** Displays microscopy and elemental distribution analysis of the material, of materials a)  $\text{Cu}_2\text{S}$ , b)  $\text{ZnO}$ , and c)  $\text{Cu}_2\text{S}/\text{ZnO}$ .

The micrographs and EDS mapping in Figure 2 reveal a uniform distribution of elements in the materials, crucial for efficient charge transfer in composite heterojunctions. This uniformity reduces recombination of photogenerated charges, enhancing photocatalytic performance. Incorporating Cu<sub>2</sub>S into ZnO creates new active sites and improves electronic conduction, showing promising catalytic properties<sup>12</sup>.

These findings suggest that the doping strategy and composite formation are effective for creating advanced photocatalysts with potential applications in environmental and energy sectors<sup>12</sup>.

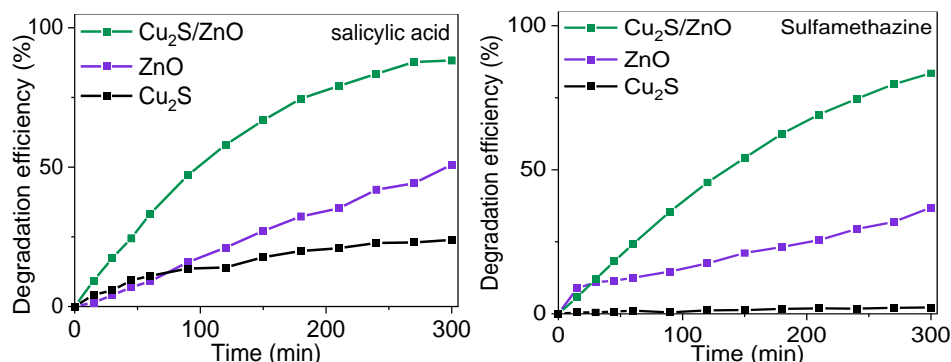


**Figure 3** Results of photocatalytic tests for the degradation of SA and AMZ

The X-ray diffractograms, FTIR and EDS, shows a strong correlation with the degradation tests presented in Figures 3, providing a comprehensive view of the photocatalyst's performance under different configurations. The figures highlight the positive impact of doping ZnO with Cu<sub>2</sub>S on catalytic performance, evident in the individual tests of each degraded compound. The structural stability indicated in the diffractograms suggests improvements in catalytic properties, resulting in enhanced outcomes in sunlight degradation tests<sup>13</sup>. The combination of Cu<sub>2</sub>S and ZnO, as shown in the diffractograms, produces more efficient materials in pollutant degradation. The consistency between the diffractograms and the degradation test results suggests that careful material selection can significantly optimize the photocatalyst's catalytic efficiency in pollutant degradation processes under sunlight irradiation<sup>14</sup>. This integrated approach between structural analysis and catalytic performance provides a solid basis for future practical applications of these materials in heterogeneous photocatalysis processes.

## 4 CONCLUSION

This study aims to investigate the effectiveness of copper-based photocatalysts, specifically Cu<sub>2</sub>S, in degrading pollutants in aquatic environments. The synthesis and characterization of these materials revealed that incorporating Cu<sub>2</sub>S into ZnO significantly enhances catalytic properties, facilitating efficient charge separation and increasing visible light absorption. X-ray diffraction patterns and FTIR spectra confirm the distinct crystalline structures of ZnO and Cu<sub>2</sub>S, and consistent degradation test results indicate high efficiency in degrading contaminants like salicylic acid and sulfamethazine. The uniform distribution of elements observed through electron microscopy and EDS mapping reinforces the effectiveness of the heterojunction in the composites, crucial for photocatalytic process efficiency. The combination of Cu<sub>2</sub>S with ZnO showed promising potential for forming new active sites and electronic conduction, suggesting that doping and composite formation strategies can be effective in creating advanced photocatalysts. These materials, evidenced by their structural properties and performance in degradation tests, provide a solid foundation for future applications in heterogeneous photocatalysis processes, contributing to the mitigation of pollutants in ecological and energy environments. The consistency between structural analyses and degradation test results validates the choice of materials and the synthesis methodology, establishing the basis for developing sustainable and innovative catalytic technologies.

## REFERENCES

- TAHIR, M. B., RAFIQUE, M. S., SAGIR, M., & MALIK, M. F. (2022). Singapore: Springer. (pp. 49-60).
- MOHAN, H. YOO, S. THIMMARAYAN, S. OH, H. S. KIM, G. SERALATHAN, K.-K. SHIN, T. 2021. Environ. Pollut. 289. 117864.
- LI, X. BAI, Y. SHI, X. SU, N. NIE, G. ZHANG, R. NIE, H. YE, L. 2021. Mater. Adv. 2. 1570–1594.
- CAI, M., WEI, Y., LI, Y., LI, X., WANG, S., SHAO, G., & ZHANG, P. (2023). 2D. EcoEnergy, 1(2), 248-295.
- JIANG, X., ZHANG, S., CHEN, S., JIANG, C., & YAO, X. (2024). Applied Surface Science, 159701.
- XU, T., WANG, P., WANG, D., ZHAO, K., WEI, M., LIU, X., & Yang, L. (2020). Journal of Alloys and Compounds, 838, 155689.
- NAWAZ, Tabish; SENGUPTA, Sukalyan. Elsevier, 2019. p. 67-114.
- SARAPAJEVAITE, G., MORSELLI, D., & BALTAKYS, K. (2022). Materials, 15(15), 5253.
- TAN, H., LI, J., HE, M., LI, J., ZHI, D., QIN, F., & ZHANG, C. (2021). Journal of Environmental Management, 297, 113382.
- Witkowski, M., Starowicz, Z., Zięba, A., Adamczyk-Cieślak, B., Socha, R. P., Szawcow, O., & Ostapko, J. (2022). Nanotechnology, 33(50), 505603.
- HAN, D., LI, B., YANG, S., WANG, X., GAO, W., SI, Z., & WANG, D. (2018). Nanomaterials, 9(1), 16.
- WANG, Z., XU, F., WANG, H., CUI, H. N., & WANG, H. (2017). Materials, 10(1), 37.
- MANI, J., RADHA, S., PRITA, F. J., RAJKUMAR, R., ARIVANANDHAN, M., & ANBALAGAN, G. (2023). Journal of Inorganic and Organometallic Polymers and Materials, 1-16.
- DE MORAES, N. P., PEREIRA, R. A., DA SILVA, T. V. C., DA SILVA, B. H. B., DE ASSIS, G. P., CAMPOS, T. M. B., & RODRIGUES, L. A. (2024). International Journal of Biological Macromolecules, 254, 127826.

## ACKNOWLEDGEMENTS

The authors would like to thank the Coordenação de Aperfeiçoamento de Pessoal de Nível Superior (CAPES) - Financing Code 001, and the São Paulo Research Foundation (FAPESP) - Process n° 2022/04058-2, and 2023/13127-0 and University of São Paulo (PUB USP Scholarships), for the financial support.